Optical excitation spectra of trapped electrons in irradiated feldspars

2003 J. Phys.: Condens. Matter 15 8011

(http://iopscience.iop.org/0953-8984/15/46/017)

INSTITUTE OF PHYSICS PUBLISHING JOURNAL OF PHYSICS: CONDENSED MATTER

J. Phys.: Condens. Matter **15** (2003) 8011–8027 PII: S0953-8984(03)65969-2

Optical excitation spectra of trapped electrons in irradiated feldspars

Marc René Baril[1] **and D J Huntley**

Department of Physics, Simon Fraser University, 8888 University Drive, Burnaby, British Columbia V5A 1S6, Canada

E-mail: marcrene@sfu.ca

Received 4 July 2003
Published 7 November 2003
Online at stacks.iop.org/JPhysCM/15/8011

Abstract

The dependence of optically stimulated luminescence spectra on the energy of excitation photons has been investigated for a wide range of feldspars. In the vicinity of the 1.44 eV resonance, the spectra are in many cases best described by a Voigt profile with a minor Lorentzian component centred at 1.44 eV. Most samples display a second excitation resonance near 1.57 eV, and more rarely a third peak at 1.3 eV. The shape of the excitation spectrum is the same for both the violet (3.1 eV) and yellow–green (2.2 eV) emission bands and, for one sample, the UV band (3.3–3.7 eV). The shape of the excitation spectrum is unaffected by the polarization direction of the excitation beam. The principal resonance at 1.44 eV broadens little, if at all, with increasing temperature over the range 290–490 K. The initial luminescence decay rate as a function of the initial luminescence intensity per unit energy was determined over a wide range of excitation energies (1.24–2.58 eV) for four feldspars. In every case, the initial slope was observed to increase linearly with the square of the initial intensity over the range 1.24–2.4 eV. All this provides strong evidence that excitation is from a single trap located at least 2.5 eV below the conduction band.

1. Introduction

Naturally irradiated feldspars exhibit luminescence when illuminated with infrared photons of ∼1.4 eV. The luminescence may be used to determine the last time of the exposure of a feldspar-bearing sediment to sunlight and forms the basis of optical dating (Huntley *et al* 1985, Aitken 1998). Potassium feldspars are particularly useful for dating due to their bright violet luminescence and the high radiation dose necessary to produce saturation of their luminescence.

Ionizing radiation, either environmental or laboratory, frees electrons from their regular atomic sites, and after thermalization some of them are attracted to, and become localized at,

[1] Author to whom any correspondence should be addressed.

0953-8984/03/468011+17$30.00

certain defects; these defects are called traps. Trapped electrons can be ejected by photons of sufficient energy, and these electrons may then de-excite at another defect with the emission of photons. This process is called optically stimulated luminescence.

Excitation spectra provide the most direct means of obtaining information about the traps involved in optically stimulated luminescence. The observation of an excitation resonance near 1.44 eV (860 nm, infrared) in feldspars was first reported by Hütt *et al* (1988). Hütt *et al* (1988) actually reported resonances at 1.29, 1.33, 1.43 and 2.25 eV, with the response heading to zero at 2.34 eV. It is clear from subsequent studies that most of the observations are experimental artifacts. What has survived is the existence of a broad resonance at 1.44 eV, and an increased response above 1.6 eV, studied by several workers (Bailiff and Barnett 1994, Bøtter-Jensen *et al* 1994, Godfrey-Smith and Cada 1996, Barnett and Bailiff 1997, Hütt *et al* 1999). Krbetschek *et al* (1997) have provided a review, and pointed out that in most studies more than one emission band was measured, and that this was not desirable.

The 1.44 eV resonance is thought to be due to a transition from the ground state to an excited state of the trap. At higher excitation energies, the luminescence is roughly exponentially dependent on the excitation energy (Ditlefsen and Huntley 1994, Bøtter-Jensen *et al* 1994). This may be interpreted as arising from excitation of the trapped electrons into levels lying just below the conduction band according to Urbach's rule, (Kurik 1971).

In this paper we present measurements of excitation spectra for a range of feldspars and a few feldspar sediment extracts. Excitation spectra were obtained for both the violet (3.1 eV) and yellow–green (2.2 eV) emission bands, and the UV (3.6–3.8 eV) bands for one orthoclase sample. The temperature dependence of the excitation spectrum was obtained for six feldspar samples. In addition, the effect of the polarization angle of the excitation beam on the excitation spectrum was investigated in one oriented microcline. A measurement of the intensity decay rate versus intensity at different excitation photon energies was performed on four feldspars to help determine whether a single trap or multiple traps are involved.

2. Samples

The feldspar samples consisted primarily of specimens obtained from Ward's supply house[2] cut into roughly 8 mm × 8 mm slices. The microcline K7 and orthoclase K3 consisted of single crystals. The rock samples were analysed for all major element contents (Si, Al, K, Na, and Ca) and many common trace elements (Ba, B, Fe, Mg, Mn, Tl, Pb, Cu, Ga, Ti, Ce, Nd, Sm, Eu, Tb, Dy)[3]. Samples AKHC, EIDS and IV-1 are potassium rich feldspar sediment extracts that have been prepared using standard density separation (e.g. Ollerhead *et al* 2001). Sample descriptions and element analyses are reported in Baril and Huntley (2003).

3. Excitation spectra

The measurement system consisted of an excitation source, which for most measurements was a tunable Ti–sapphire laser pumped by a 6 W argon-ion laser, and a measurement chamber to collect and count the luminescence photons (figure 1). The energy range of the excitation photons was 1.24–1.77 eV (700–1000 nm). Light collection was provided by an ellipsoidal mirror with the sample placed at one focus of the ellipsoid and an EMI 9635Q photomultiplier tube (PMT) placed at the second focus, Baril (1997). The excitation beam was admitted

[2] Ward's Natural Science Ltd, 397 Vansickle Road, St Catherines, Ontario.

[3] Analyses were performed by Acme Analytical Laboratories Ltd, 852 East Hastings Street, Vancouver, BC V6A 1R6.

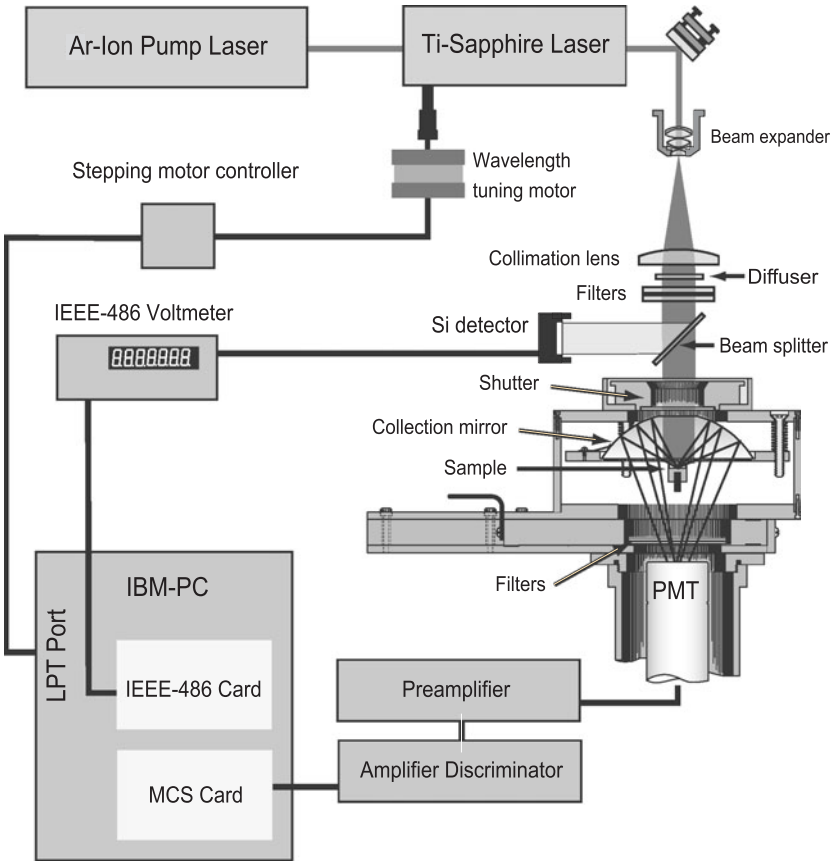

Figure 1. Setup for measuring excitation spectra.

through a 3 cm diameter hole in the centre of the ellipsoidal mirror. Filters placed before the PMT absorbed the scattered excitation photons while allowing the selected luminescence band to be measured. The emission bands were selected using the following filter combinations.

- Yellow–green (2.2 eV): two 2.2 mm thick Schott BG-39 filters and one 3.1 mm thick Schott OG-530 filter.
- Violet (3.1 eV): two 2.2 mm thick Schott BG-39 filters and one Kopp 7-59 filter.
- UV (3.3–3.7 eV): two 3.0 mm thick Schott UG-11 filters and one BG-39 filter.

The beam power was monitored using a thin glass beam-splitter. No correction was made for the variation in the reflectance of the beam-splitter over the excitation range because the total variation was less than 5% and very gradual. The luminescence intensity was divided by the average beam power recorded during the illumination period and multiplied by the excitation photon energy to yield the ratio of the number of detected luminescence photons to the number of incident excitation photons. A holographic diffuser was placed in the excitation beam to avoid strong diffraction patterns forming at the sample due to the beam-splitter and to ensure a broad, uniform illumination of the sample.

Samples were bleached under a halogen lamp fitted with a 2 mm thick RG-715 filter for 3 h and then given a ∼1500 Gy gamma dose. Samples were preheated for 16 h at 120 °C

after removal from the gamma source; storage times prior to measurement varied from hours to several days.

A single aliquot was used for the measurement of an excitation spectrum. The aliquot was typically illuminated for 3 s at each wavelength, with a laser beam power of typically 10–100 μW cm^{-2}. A measurement at the initial excitation wavelength was repeated at the end of the scanning sequence to determine the amount of luminescence decay that occurred during the scan. Generally, the decay was well below 10%, so no correction for the decay was made.

Acquisition of the full 1.24–1.77 eV (700–1000 nm) excitation band required the insertion of three separate optic sets into the Ti–sapphire laser. Each excitation spectrum therefore represents the combination of three spectra for the ranges 1.24–1.35 eV (915–1000 nm), 1.35–1.65 eV (750–915 nm) and 1.65–1.77 eV (700–750 nm).

The excitation spectra for the yellow–green band were scaled to the maximum response of the violet emission and are shown along with the violet emission excitation spectra in figure 2. The bold curve in these diagrams represents a fit using a Voigt profile for the principal resonance, a Gaussian for the secondary resonance near 1.57 eV and an exponential rise at high energy (equation (4)). The fine line curves represent the individual Voigt, Gaussian and exponential terms in the fit. The fits are described in section 5.

4. The excitation spectra: general observations

The excitation resonance maximum occurs near 1.44 eV in most samples, irrespective of nominal composition (table 1). The position of the resonance maximum did not differ by more than 0.01 eV from 1.442 eV in any of the samples using a fit to equation (4). In many samples the resonance appears to have a Lorentzian character with varying amounts of asymmetric broadening. The asymmetry arises from a secondary resonance near 1.57 eV.

For samples A2 and K3 (the only samples for which complete excitation spectra for two emission bands were measured) the excitation spectra for the violet and yellow green bands in A2, and the violet and UV bands in K3 are in excellent agreement. For all samples the excitation spectra for the yellow–green emission is not significantly different from that for the violet emission, although in a few samples (in particular A5 and K10) the resonance appears to be somewhat broader for the yellow–green emission than that seen in the violet band. In some samples (e.g. K7 and K8) the response peak for the yellow–green emission is shifted slightly from that observed for the violet emission. There is strong evidence that in sample K8 the violet and yellow–green emission originates from different mineral phases in the crystal so that the large difference in the excitation spectra for the two bands is not entirely surprising in this sample, (Baril 2003).

These results differ significantly from those of Godfrey-Smith and Cada (1996) in that a much more idealized absorption line-shape is obtained in the present case. In addition, Godfrey-Smith and Cada report a resonance maximum at 1.46–1.48 eV whereas in the present study it is closer to 1.44–1.45 eV. The shape of the long wavelength wing of the 1.44 eV resonance in the data of Bøtter-Jensen *et al* (1994) is highly dependent on feldspar composition; this contrasts sharply with the present results which indicate a minimal dependence on the variety of feldspar measured. The maximum emission occurs at 1.44 eV in their Na and K-feldspar samples, in agreement with our study. The present excitation spectra are generally consistent with those of Barnett and Bailiff (1997). The resonance maximum does not deviate by more than 0.017 eV from 1.443 eV in their 15 samples. A Lorentzian character to the resonance is not evident in any of their samples, perhaps due to the lack of points on the low energy wing of the resonance. In addition, the decrease at higher energies observed in their data is more dramatic than in the data presented here. Barnett and Bailiff obtain satisfactory fits using a sum of two Gaussians, whereas this is rarely true for our samples.

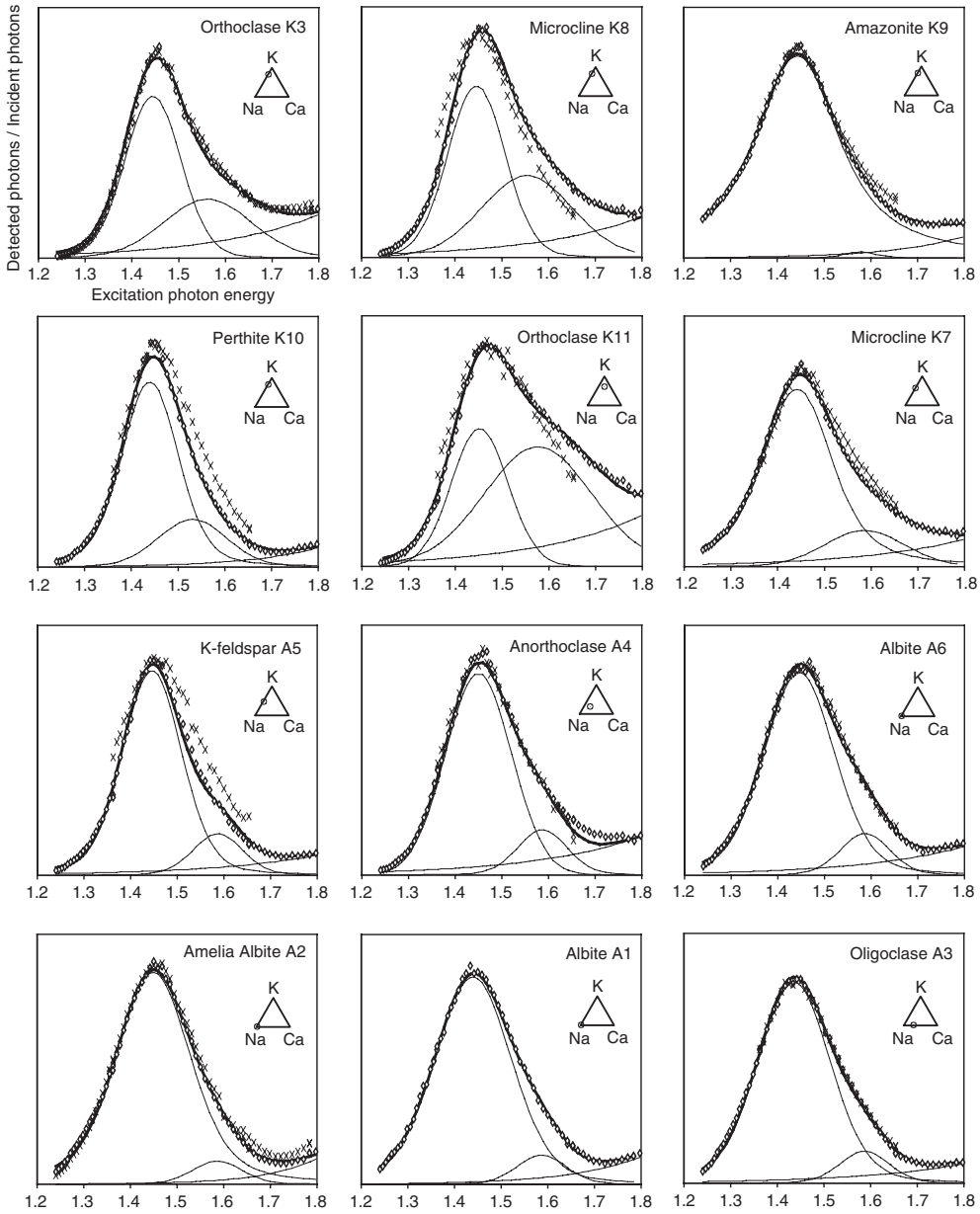

Figure 2. Excitation spectra for the feldspar samples. Open diamonds are for the violet emission band, crosses represent the yellow–green emission band—except for sample K3, where they represent the UV band measurement. The bold curve is a fit to the violet emission data using a Voigt profile for the principal resonance, a Gaussian near 1.57 eV and an exponential; these three components are shown by the fine curves. The solid circles on the triangle indicate the proportions of K, Na, and Ca from the analyses.

It is worth noting that the potentially important effect of the optical absorption of the samples has not been taken into account in this experiment. The absorption varies relatively smoothly over the excitation band 1.2–1.8 eV, but is highly sample dependent (Hofmeister and

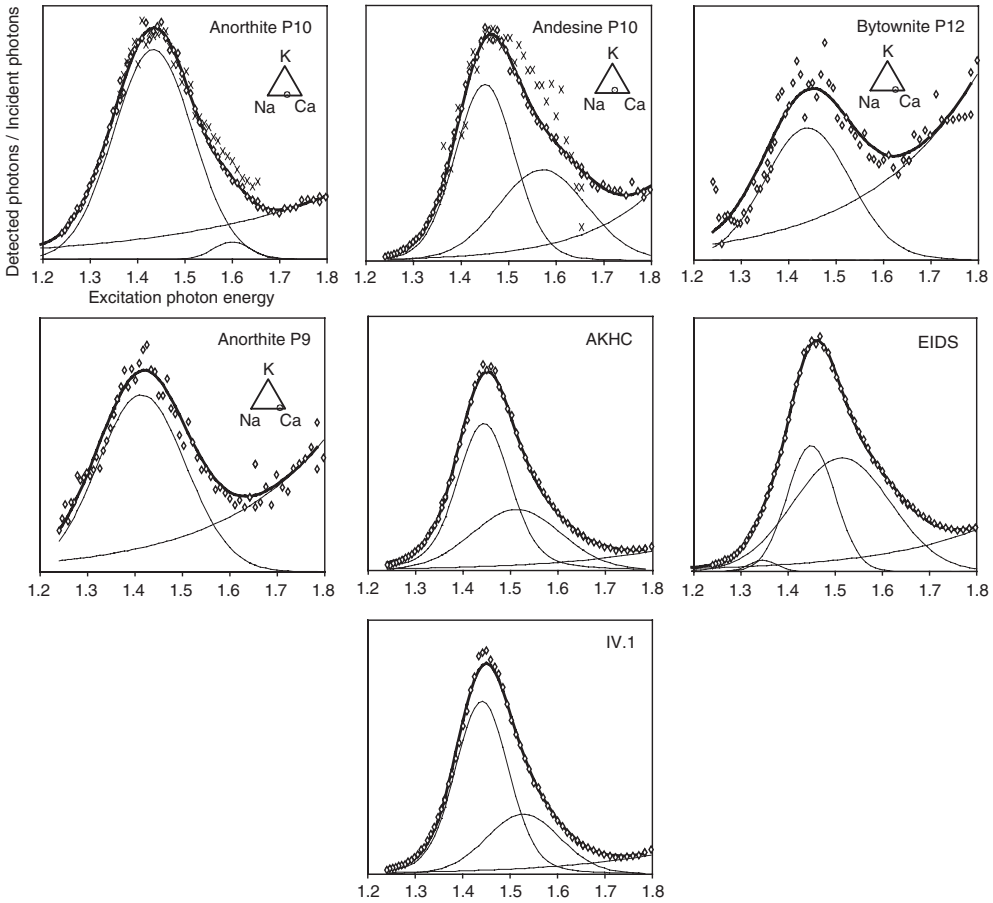

Figure 2. (Continued.)

Rossmann 1984). The problem of correcting for the absorption is complicated because it depends on the depth of the excited luminescence in the sample slice or grains. Since our samples are rarely of uniform optical quality, application of a correction for absorption is not practical.

5. Fits to the excitation spectra: interpretation of the line-shape

Fits of the excitation spectra to various combinations of Gaussian, Lorentzian and Voigt peaks were attempted with the aim of finding some common behaviour among the samples. In particular it was hoped that the position of the resonances in the excitation spectrum would be more or less consistent between samples. The high-temperature excitation spectra (section 5.1) clearly indicated the presence of an additional resonance near 1.3 eV, that is rarely evident in the samples at room temperature. With this in mind, a fit was made using three Gaussians and an exponential. Good fits were obtained for all the samples. However, in several samples the positions of two of the three Gaussian peaks almost coincided, departing strongly from the expected position of the hypothetical resonances at 1.3, 1.4 and 1.6 eV. This was taken as an indication that the fitting function was incorrect. Samples such as A1, A5, K7, K9, K10, AKHC and IV.1 appear to exhibit a significant Lorentzian character in the principal resonance

Table 1. Peak positions for the two fits to the excitation spectra ('Gaussian fits': three Gaussians + an exponential. 'Voigt + Gaussian fit': Voigt profile + Gaussian + exponential). $\Delta\epsilon_{0(L)}$ and $\Delta\epsilon_{0(G)}$ are the widths of the Lorentzian and Gaussian components of the Voigt profile. $\Delta\epsilon_1$ is the width of the 1.57 eV Gaussian. All values are in electronvolts.

	Gaussian fits			Voigt + Gaussian fit (equation (4))				
Sample	ϵ_0	ϵ_1	ϵ_2	ϵ_0	$\Delta\epsilon_{0(L)}$	$\Delta\epsilon_{0(G)}$	ϵ_1	$\Delta\epsilon_1$
A1	1.432	1.46	1.34	1.440	0.037	0.173	1.59	0.11
A2	1.445	1.58	1.31	1.449	0.068	0.149	1.59	0.16
A3	1.427	1.55	1.32	1.436	0.029	0.167	1.59	0.10
A4	1.446	1.52	1.36	1.450	0.002	0.164	1.59	0.14
A5	1.437	1.50	1.32	1.446	0.029	0.133	1.57	0.14
A6	1.449	1.59	1.29	1.446	0.036	0.158	1.58	0.12
K3	1.444	1.55	1.34	1.445	0.010	0.136	1.56	0.21
K7	1.451	1.48	1.42	1.442	0.086	0.125	1.59	0.19
K8	1.446	1.54	1.34	1.446	0.010	0.139	1.55	0.22
K9	1.439	1.45	1.35	1.443	0.177	0.085	1.58	0.07
K10	1.441	1.60	1.45	1.440	0.036	0.123	1.53	0.16
K11	1.453	1.57	1.32	1.452	0.002	0.141	1.58	0.26
P9	1.412	—	—	1.414	0.005	0.216	—	0.24
P10	1.433	1.60	—	1.433	0.056	0.172	1.58	0.13
P11	1.447	1.56	1.34	1.450	0.016	0.138	1.57	0.21
P12	1.444	1.49	—	1.440	0.013	0.205	—	0.22
AKHC	1.444	1.51	1.34	1.444	0.040	0.110	1.51	0.21
EIDS	1.449	1.48	1.35	1.448	0.020	0.139	1.56	0.20
IV.1	1.443	1.48	1.40	1.441	0.025	0.188	1.53	0.17

(a sharp peak with broad wings). This line-shape may be approximated by two Gaussians of different widths centred at the same energy. For this reason, we suggest that the Voigt profile provides a more meaningful description of the resonance as described below.

The Lorentzian line-shape is most commonly associated with the fundamental width of a radiative transition. This arises from the uncertainties of the energies of the initial and final states due to the lifetime of the state. The spectral intensity is written as

$$I(\epsilon) \propto \frac{(\hbar\gamma/2)^2}{(\epsilon - \epsilon_0 - \Delta)^2 + (\hbar\gamma/2)^2} \tag{1}$$

which is the familiar Lorentzian absorption/emission line-shape. The transition rate peaks at the photon energy ϵ equal to the energy difference ϵ_0, between the electronic ground and excited states, shifted by a small energy Δ. The latter is effectively the Lamb shift and is usually neglected. The line width (full-width at half maximum, or FWHM) is given by $\Delta\epsilon = \hbar\gamma/2$, where γ is the decay rate from the excited state (i.e. the inverse of the mean life τ of the excited state, $\gamma = 1/\tau$).

A Lorentzian line-shape can also arise from any number of time-dependent perturbations so that in practice the line width $\Delta\epsilon_L$ consists of the sum of the contributions from various sources (Di Bartolo 1968). In the case of a crystal, the 'intrinsic' line width discussed above is usually overshadowed by other effects producing Lorentzian profiles. The most common of such effects is the Raman scattering of phonons at the radiating (or absorbing) centre; that is, the absorption of a phonon and the emission of another phonon by the radiating 'ion'. In this case, the time over which the perturbation evolves (i.e. the period of a lattice vibration) is much longer than the transition time so that the perturbation of the energy levels is effectively constant over the transition interval.

Gaussian line-shapes generally arise from completely different processes. The profile may be thought of as arising from the superposition of a large number of spectral lines, with each line representing the energy level of a particular group of radiation centres. For example, in a crystal the levels of a particular emitting/absorbing ion will vary throughout the lattice due to local variations in the crystal field caused by nearby defects. If the defects are spatially random, then the spectral line will consist of the superposition of numerous lines at different energies. It is reasonable to expect that numerous types of defects are present in the crystal, furthermore, the density and distance of these defects from the emitting/absorbing centre are also likely to vary greatly. In such a case, the distribution of energy levels for the centre depends on the sum of a large number of independent random variables so that the resulting energy distribution is Gaussian[4].

The observed line-shape is then a convolution of Lorentzian and Gaussian probability distributions called the Voigt profile, Di Bartolo and Powell (1976),

$$f_{\mathrm{v}}(\epsilon) = \frac{2\ln 2}{\pi\sqrt{\pi}}\frac{\Delta\epsilon_{\mathrm{L}}}{\Delta\epsilon_{\mathrm{G}}^2}\int_{-\infty}^{+\infty}\frac{\mathrm{e}^{-\xi^2}}{a^2+(b-\xi)^2}\,\mathrm{d}\xi$$
$$a = \frac{\Delta\epsilon_{\mathrm{L}}}{\Delta\epsilon_{\mathrm{G}}}\sqrt{\ln 2}, \qquad b = \frac{2(\epsilon-\epsilon_0)\sqrt{\ln 2}}{\Delta\epsilon_{\mathrm{G}}} \tag{2}$$

where $\Delta\epsilon_{\mathrm{G}}$ and $\Delta\epsilon_{\mathrm{L}}$ are the Gaussian and Lorentzian line widths respectively and ϵ_0 is the centre frequency. In the limit $\Delta\epsilon_{\mathrm{G}} \to 0$, the Lorentzian line-shape is obtained, whereas the Gaussian line-shape is recovered when $\Delta\epsilon_{\mathrm{L}} \to 0$.

Raman scattering by phonons can cause Lorentzian broadening, Di Bartolo and Powell (1976). This phonon interaction has a strong dependence on temperature and contributes a width $\Delta\epsilon_{\mathrm{L}}$ to the transition,

$$\Delta\epsilon_{\mathrm{L}} = \bar{\alpha}\left(\frac{T}{\Theta_{\mathrm{D}}}\right)^7\int_0^{\frac{T}{\Theta_{\mathrm{D}}}}\frac{\xi^6\mathrm{e}^{\xi}}{(\mathrm{e}^{\xi}-1)^2}\,\mathrm{d}\xi \tag{3}$$

where Θ_{D} is the Debye temperature and $\overline{\alpha}$ is a constant that depends on the phonon scattering cross-section. However, as is shown later, there is little or no effect of temperature on the width of the excitation resonance so we conclude that this effect is not significant.

The previous analysis of the excitation spectrum has been in terms analogous to regular absorption and emission lines in a crystal. This may not be appropriate since there are processes occurring between excitation and emission that are as yet not established. The similarity of excitation spectra for different emission bands is an indication that such processes do not play a role in the line width.

Since the luminescence is proportional to the excitation flux at fixed temperature, the model function for the luminescence response must only contain additive, photon-energy dependent terms. The following model function is proposed,

$$I(\epsilon) \propto A_0 f_{\mathrm{v}}(\epsilon, \epsilon_0, \Delta\epsilon_{0(\mathrm{L})}, \Delta\epsilon_{0(\mathrm{G})}) + A_2\mathrm{e}^{+S\epsilon} + A_1\exp\left(-4\ln 2\left[\frac{\epsilon-\epsilon_1}{\Delta\epsilon_1}\right]^2\right) \tag{4}$$

where f_{v} is the Voigt distribution function as above and $S = \sigma(T)/kT$ (if Urbach absorption is applicable). The third term is a secondary resonance, required to obtain satisfactory agreement with the data; a Gaussian line-shape was selected for simplicity, but in general it should be described by a Voigt distribution.

Equation (4) fits the excitation spectra almost as well as the sum of Gaussians described earlier; the parameters determined for the two fits are shown in table 1. The position of the secondary resonance near 1.57 eV strays very little between samples using the Voigt fit

[4] This result is due to the central limit theorem.

compared to the fit using three Gaussians. Samples K9 and K10 illustrate this best, although the Voigt profile cannot adequately fit points near the excitation maximum, it does so far better than a single Gaussian. The poor fit of the Voigt curve near the resonance maximum in K9 and K10 can be resolved by introducing an additional resonance near 1.3 eV. However, data extending to lower excitation energies would be required to allow a statistically meaningful fit using this additional resonance.

The width of the resonance inferred from the fits varies little from sample to sample, being in the range 0.13–0.19 eV at room temperature. The Gaussian component is dominant, thus we expect the width to arise from defects near the absorbing centre. The samples, however vary widely in composition, structure and appearance, and are unlikely to have similar defect contents. This puzzle remains unsolved.

In all but one sample (K9) the Gaussian component of the Voigt profile is found to dominate. It would be instructive to see whether the relative contribution from the Lorentzian component correlates with the obliquity of the samples, which is a measure of the ordering of Si–Al atoms in the lattice. 'Sanidinized' microcline, that is microcline (high Si–Al order) that has been heated so that its structural phase changes to sanidine (no Si–Al order) would be useful for this purpose. It is clear however, at least from our data, that no generalizations can be made as to the relative contributions of the Gaussian and Lorentzian components to the excitation resonance for samples of a given nominal composition.

5.1. Temperature dependence of the excitation spectra

Excitation spectra were measured for orthoclases K3 and K11, albites A2 and A5, and microclines K9 and K10 for temperatures from 290 to 490 K. Samples were first heated for 20 h at 200 °C to reduce any thermoluminescence background to a negligible value. A single aliquot was used for the excitation spectra for a given sample, using an excitation power that produced less than 2% decay per spectrum. Spectra were measured in order of increasing temperature, thus the intensity at higher temperature may be slightly underestimated. The excitation spectra are shown in figure 3. Varying amounts of broadening of the principal excitation resonance with increasing temperature were observed in all the samples. In K3 and K9 the broadening is strongly asymmetric. In the case of K9 the asymmetric broadening is only satisfactorily explained by the presence of an additional resonance near 1.32 eV. Subsequent fits to the spectra using three Gaussians and an exponential were consistent with the existence of a resonance near 1.34 eV in four samples (A5, K9, K10, K11). These fits were used to separate out the temperature dependence of the three observed resonances and the exponential term; the Arrhenius plots are shown in figure 4.

It should be noted that the fits did not completely separate out the three resonances, especially in sample A5; this is likely due to the approximation of the principal (Voigt) peak by a Gaussian. For this reason, the position of the peaks was determined for the higher temperature excitation spectra (where the resonances at 1.34 and 1.57 eV were most prominent) and forced to remain within 0.02 eV of the high temperature values in the fits to the lower temperature spectra. For these reasons, the results must be interpreted with some caution.

Nevertheless, certain conclusions may clearly be drawn from the results of these fits. The increase of the luminescence with temperature in samples A5 and K10 exhibited strong departures from the usual Arrhenius law, with the luminescence appearing to reach a plateau above 470 and 430 K respectively. Similar departures from the Arrhenius law at high temperature are evident in samples A5, K11 and K9; the thermal activation energy E_{th} is lower at higher energy for all three resonances. In samples A2 and K3, the departure is in the opposite direction, with a higher E_{th} at higher temperature. It should be noted that one cannot

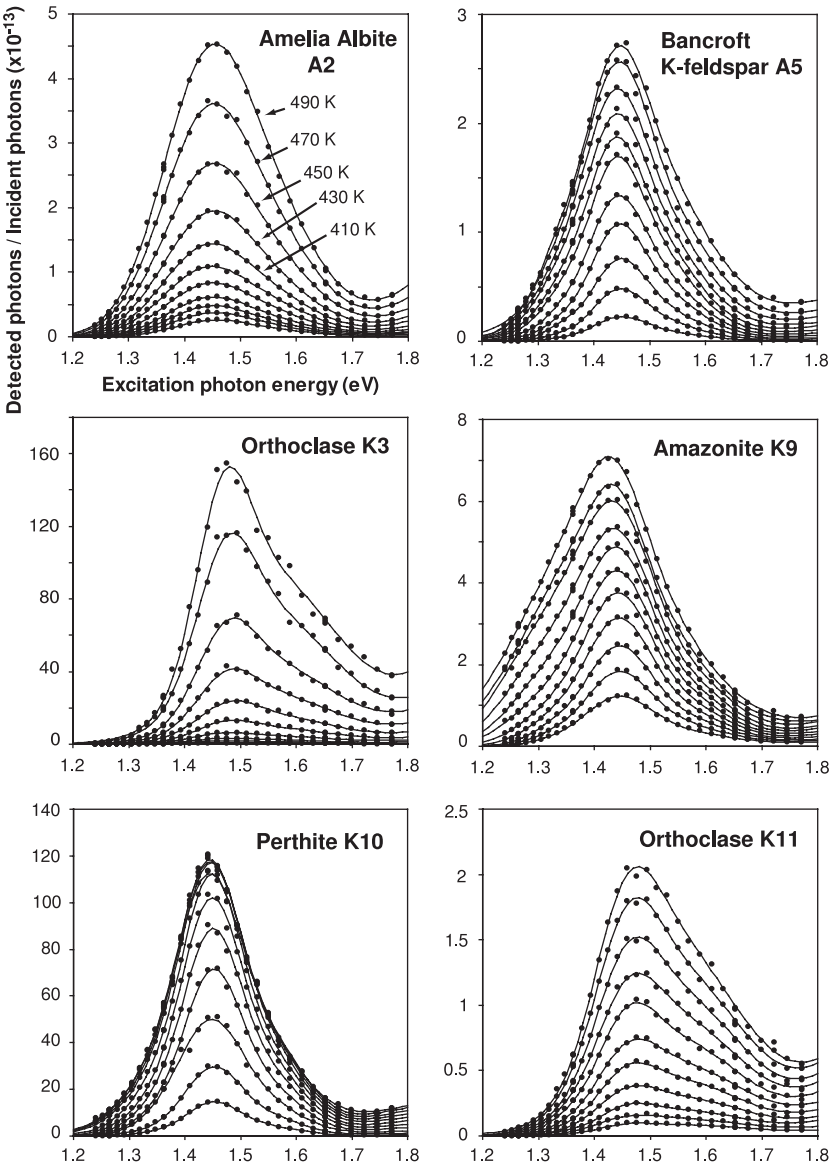

Figure 3. Temperature dependence of the excitation spectra for temperatures between 290 and 490 K. Each curve represents a 20 K increment in temperature. Solid curves are fits through the data using three Gaussians.

attach too much significance to the intensity of the exponential term because of the ignored contribution from a resonance at 2.0 eV to the exponential term in our fits.

An uncritical view of the main resonance of K9 shows its width increasing with temperature. Analysis of the data shows this to be an artifact arising from the fast rise of the 1.32 eV resonance. The width of the 1.44 eV resonance is actually nearly constant; figure 5 gives its width as a function of temperature for all six samples, and we conclude that there is little or no temperature dependence of the width of the 1.44 eV resonance. The implication of this is that phonons do not play any role in determining the width.

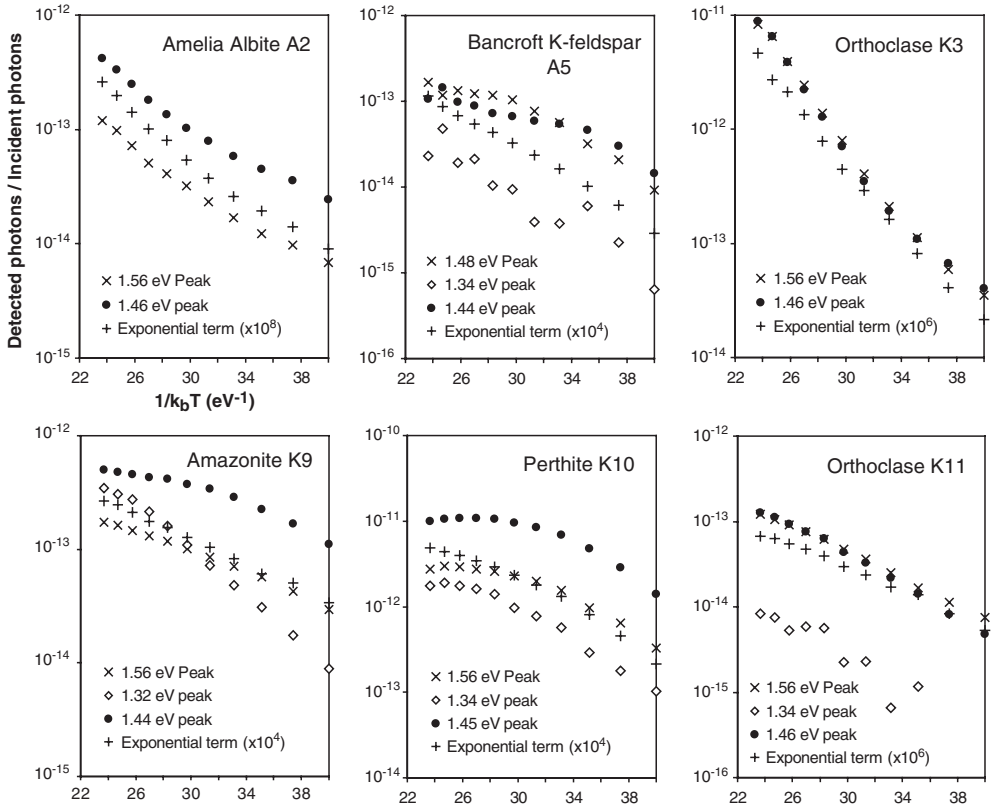

Figure 4. Arrhenius plots of the peak intensities from fits to the excitation spectra (290–490 K).

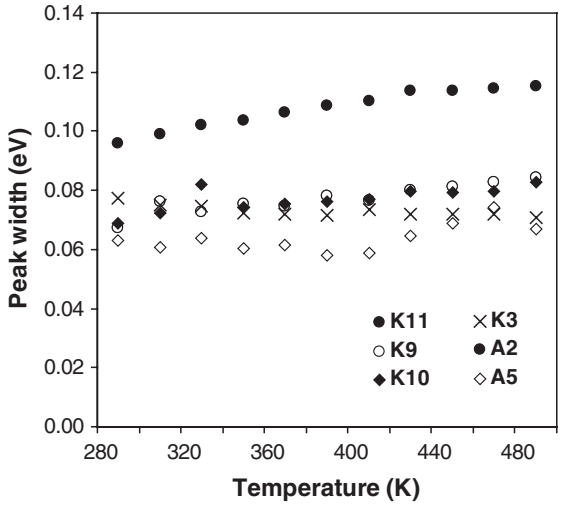

Figure 5. Peak width of the resonance near 1.44 eV as calculated from the Gaussian fits.

Figure 4 shows Arrhenius plots for the individual components of the excitation spectra. If instead, one makes Arrhenius plots of the actual data and from their slopes determines

a thermal activation energy, E_{th}, as a function of incident photon energy, one can expect a complex result which is not obviously meaningful. This procedure was used by Poolton *et al* (1995), who found a minimum in E_{th} at $\sim$1.44 eV. We can now see that this is an artifact arising from the temperature dependences of the 1.34 and 1.57 eV resonances being higher than that of the 1.44 eV resonance. Two of our samples, A5 and K10, exhibit this behaviour. When the temperature dependences are the same for the different contributions (e.g. A2 and K3) no minimum exists.

The value of E_{th} for the 1.44 eV resonance obtained from an Arrhenius plot ranges from 0.20 eV near room temperature to 0.42 eV at temperatures above 380 K. This last value is much larger than is typically found in the literature; it is also larger than the value of 0.151 ± 0.002 eV found by Short (2003) for the same sample over the temperature range 310–410 K. The difference appears to be the result of the heating used in the present experiment.

5.2. Effect of polarization on the excitation spectrum

It has been found by Short and Huntley (2000) that the intensity of the violet emission of orthoclase K3 is dependent on the polarization of the excitation light. In addition, K3's violet emission is also polarized. The observations are consistent with dipole transitions, with a dipole aligned close to the [113] crystal direction in both cases. One question of interest is whether the excitation spectrum is dependent on the polarization of the exciting light. Microcline K7 was convenient for detailed study since its growth habit allowed a simple means by which to determine its orientation.

The experimental setup was identical to that described earlier with the inclusion of a Fresnel-Rhomb 1/2-wave plate in the excitation beam path to allow rotation of the polarization of the excitation. The effect of the polarization direction of the excitation beam on the violet luminescence band intensity of K7 for 1.44 eV excitation is shown in figure 6. The dependence was measured for two thin crystal slices cut parallel to the (001) (slice-C) and (010) (slice-B) planes and is generally consistent with the measurement by Short and Huntley (2000) on orthoclase K3.

The excitation energy response for the violet emission band was measured for an excitation beam perpendicular to (001) (slice-C) at different polarization orientations (figure 7). No significant change in the shape of the excitation energy response was observed as the excitation polarization was varied, aside from the previously noted uniform change in intensity.

One should note that the connection between the polarization direction of the excitation and the orientation of the presumed dipoles is non-trivial due to the ubiquitous birefringence of feldspars. In general, several assumptions have to made in deducing the orientation of the emitting or absorbing dipoles from data like that of figure 6, Short and Huntley (2000). Some of these assumptions involve knowledge of the optical axes of the crystal; these have not been determined for K7.

6. Initial decay rate versus initial intensity: a single trap?

The question we address here is whether a single type of trap or two or more types of trap are involved in the optically stimulated luminescence of feldspars.

On the basis of the existence of several peaks in their excitation spectra Hütt *et al* (1988) suggested that there are several traps. This must now be discounted because some aspects of their data are spurious. On the basis of similar dose response Hütt *et al* suggested that the 1.43 and 2.25 eV excitation bands were associated with the same trap. Models used to explain the various luminescence data generally include more than one trap (e.g. McKeever

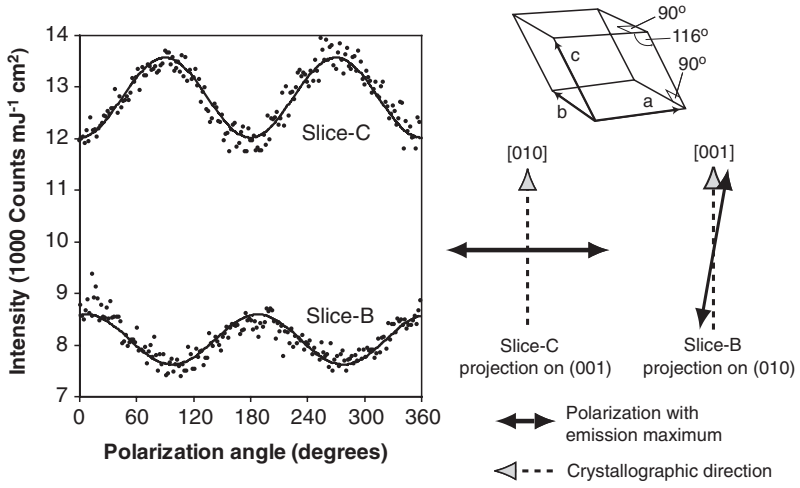

Figure 6. Left: the effect of the polarization of the excitation on the emission intensity in microcline K7. Slice-C was cut parallel to (001) and 'slice-B' was cut parallel to (010). The solid curves are fit through the data. The polarization angle is measured with respect to [010] for slice-C and [001] for slice-B. Right (top): geometry of monoclinic feldspar unit cell. Right (bottom): diagram of the relevant directions for the slice-C and slice-B measurements (note that the directions shown do not necessarily lie in the plane of the page).

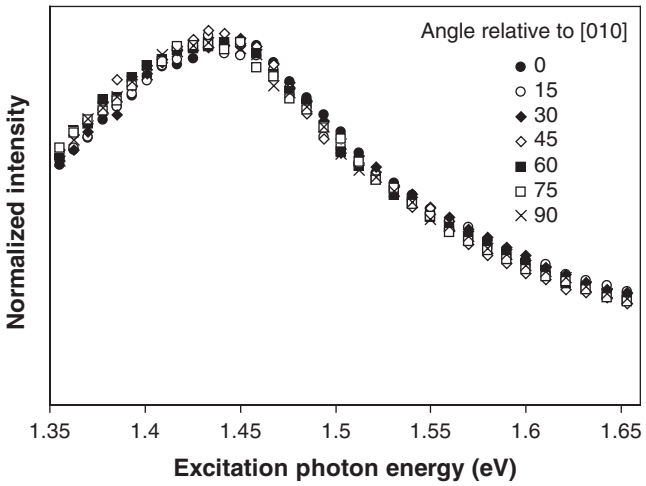

Figure 7. Effect of the polarization direction of the excitation photons on the excitation spectrum of K7 (violet emission band). The polarization direction producing maximum violet emission is parallel to [010]; the spectrum for this orientation is labelled '0°'. All other excitation spectra have been scaled so that the intensities roughly coincide with those of the 0° spectrum. Angles are measured with respect to the 0° orientation. Excitation spectra from 105° to 180° have been averaged with those from 0° to 75° to simplify display.

et al 1997) though Trautmann *et al* (2000) found that for radioluminescence and optically stimulated luminescence, only one trap is necessary.

Ditlefsen and Huntley (1994) approached this problem by looking at how the initial intensity per unit energy $I_0(J)$ scaled with the rate of decay per unit energy, $S_0(J)$. Here,

J is the integrated photon energy incident on the sample,

$$J = n\hbar\omega t \tag{5}$$

where t is time, $\hbar\omega$ is the photon energy (a monochromatic source is assumed) and n is the rate per unit area at which photons are incident upon the sample.

In the simplest case one expects that the excitation probability depends on the energy of an incident photon, but that once excited, the fate of an electron is completely independent of the excitation process. In this case one can expect the intensity,

$$I(J) \propto f(J/J_0) \tag{6}$$

with J_0 being a parameter dependent on the incident photon energy. Assuming that the total integrated intensity has a fixed value, it is readily shown that the initial rate of decrease of intensity is proportional to the square of the initial intensity, I_0.

$$S_0 \equiv \left.\frac{\mathrm{d}I(J)}{\mathrm{d}J}\right|_{J=0} \propto I_0^2. \tag{7}$$

For example, exponential (first-order) decay follows the form of equation (6)

$$I(J) = I_0 \mathrm{e}^{-J/J_0} \tag{8}$$

where, in this case, J_0 is connected to the cross-section, σ, for excitation out of the trap by $J_0 = \hbar\omega/\sigma$. In the case of multiple traps exhibiting first-order decay, the luminescence intensity would follow a sum of decaying exponentials with a different J_0 for every trap (i.e. depending on the individual trap cross sections σ), and the scaling $S_0 \propto I_0^2$ would not hold. With multiple traps and non-exponential decays where J_0 is connected to a trap parameter, it would also not hold.

Ditlefsen and Huntley (1994) tested this relation for excitation energies ranging from 1.77 to 2.54 eV for one quartz sediment extract, one feldspar sediment extract and two undifferentiated 4–11 μm sediments. A linear relationship between I_0 and $\sqrt{S_0}$ was observed for the quartz sample; for the others a strongly non-linear relation was obtained. Ditlefsen and Huntley's measurements did not extend below 1.77 eV, so they were unable to test this scaling in the vicinity of the excitation resonance. This region is of particular concern because one would like to know whether the excitation at different parts of the 1.44 eV resonance samples the same traps, and whether or not the excitation at higher energies, above 2 eV, samples additional traps. It is also important to do the measurements on single crystals or at least feldspar rocks. Ditlefsen and Huntley's samples were polymineralic which could have contributed to the observed lack of scaling.

Slices of the orthoclase K3 and the microclines K8, K9 and K10 were cut and bleached under a sun lamp fitted with a 630 nm cut-off, long pass filter for 70 h. The slices were given a γ dose of 800 Gy followed by a preheat at 120 °C for 16 h. Their violet luminescence was measured under brief exposure to 1.43 eV laser excitation to normalize the data later. The violet emission band was selected by using three 4 mm thick Corning 5-58s, one Corning 7-51, a single Schott 2.2 mm thick BG-39 filter and detected using an EMI 9635QB PMT.

Several light sources were used to provide the excitation. For this reason care was taken to ensure that the sample illumination was very broad and uniform. Photon energies from 1.24 to 1.77 eV were obtained using a tunable Ti–sapphire laser. Measurements at 2.54 eV (488 nm), 2.50 eV (496 nm), 2.47 eV (501 nm) and 2.41 eV (514 nm) were made using an argon-ion laser operated in single line mode. Points at 1.96 eV (632.8 nm) were obtained using a He–Ne laser, whereas those at 2.1 eV (589 nm) and 2.27 eV (546 nm) were provided using a Na-lamp/Na-doublet filter and a Hg-lamp/546 nm narrow-band filter combination, respectively.

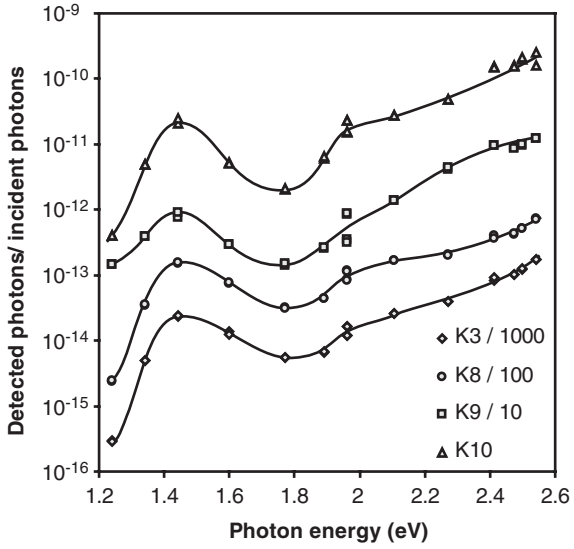

Figure 8. Initial intensity as a function of excitation energy for feldspar rock samples K3, K8, K9 and K10. Solid curve is an arbitrary curve through the data to aid visualization. Data for the different samples have been shifted along the ordinate axis for clarity.

The 1.89 eV (656 nm) source consisted of a tungsten filament lamp combined with a narrow band line filter centred on the Hα emission line.

When using the laser sources the excitation power was monitored using a calibrated silicon photo-diode detector and a beam-splitter pick-up. The beam-splitter was calibrated for the wavelength dependence of its reflectivity. For the lamp sources, the excitation power was measured before and after the measurement at the sample position. For these measurements, the power was found to vary by less than 3% over the measurement period.

The initial intensity as a function of excitation energy is shown in figure 8. In addition to the excitation resonance at 1.44 eV a smaller peak is present near 2 eV; this second 'resonance' was also evident in the data of Ditlefsen and Huntley (1994) and Bøtter-Jensen *et al* (1994). For energies above 2 eV, the increase in the luminescence is roughly exponentially dependent on the excitation photon energy.

The initial intensity expressed in PMT counts per unit excitation energy versus the square root of the initial slope is shown in figure 9 for the four samples. These plots are remarkably linear up to relatively high excitation energy, $\sim$2.4 eV, in all four samples. More significantly, the linear behaviour is particularly good in the region of the infrared excitation resonance. This result is encouraging because it suggests a simpler picture than that indicated by the preliminary work of Ditlefsen and Huntley (1994). The fact that the slope of the line through the $\sqrt{S_0}$ versus I_0 graph for each sample does not exactly cross through 0 requires investigation.

Although these results provide strong evidence against multiple traps, it is not entirely conclusive because the connection of the parameter J_0 to the trap parameters (e.g. its photo-ionization cross-section) has not yet been established for the case of Becquerel-like decay. However, these findings unambiguously rule out any model involving multi-exponential decay.

The fact that the scaling $S_0 \propto I_0^2$ holds through the weaker resonances at 1.57 and 2 eV is strong evidence that these are due to the same trap connected with the 1.44 eV resonance; the implication is that these arise from additional excited levels of the same trap.

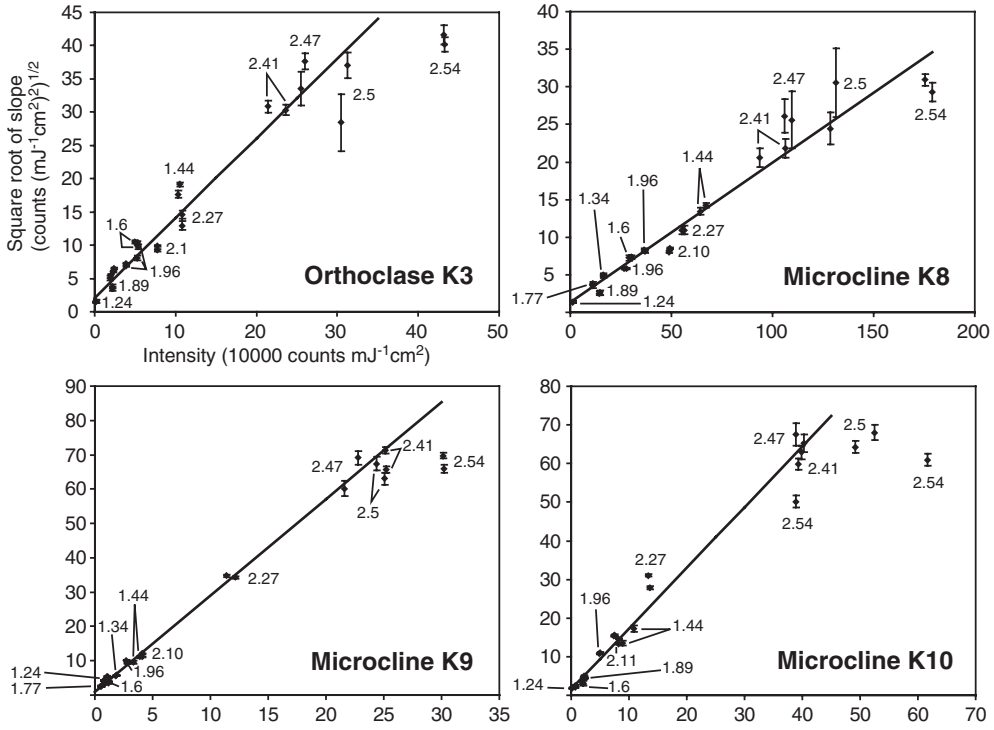

Figure 9. Square root of initial absolute slope against initial intensity for orthoclase K3 and microclines K8, K9 and K10. Labels by the points represent the photon energy of the excitation light in electron volts used to obtain the respective point.

The exponential increase of the initial luminescence intensity with the excitation photon energy above 2 eV is akin to what has been found in quartz (Huntley *et al* 1996, Ditlefsen and Huntley 1994) and may be interpreted as excitation below the conduction band (Urbach). Direct excitation to the conduction band would result in a $\sqrt{\epsilon - \epsilon_c}$ dependence on the initial intensity, where ϵ_c is the optical trap depth. The results imply that the optical trap depth must exceed 2.5 eV; this is in sharp contrast with the 2 eV optical trap depth suggested by Poolton *et al* (1994).

7. Conclusion

Investigation of the excitation energy response of the luminescence in feldspars indicates very similar behaviour among a wide range of nominal compositions. In addition, the excitation spectra are not significantly different for either the violet (3.1 eV) or yellow–green (2.2 eV) emission bands, as well as the UV bands in sample K3. This appears to indicate that for these emission bands, the recombining electrons originate from the same trap. In all cases, a maximum in the excitation response spectrum appears at 1.44–1.45 eV whose shape is best described by a Voigt profile. A weaker secondary resonance appears at slightly higher energy (∼1.57 eV), its relative contribution being highly sample dependent. A third, lower energy resonance (∼1.3 eV) becomes apparent in some samples upon heating above room temperature.

The temperature dependence of the excitation spectrum over the range 290–450 K is largely explained by the different temperature dependences of the three resonances making up

the infrared resonance. The width of the 1.44 eV resonance is approximately constant over this temperature range if the effect of the resonances near 1.57 and 1.32 eV on the excitation spectrum are accounted for.

The effect of the polarization of the excitation on the luminescence in microcline K7 was found to be in close agreement with observations made previously on orthoclase K3, Short and Huntley (2000). This may be interpreted as an indication that the orientation of the excitation dipole is identical in both feldspars. The excitation polarization direction does not appear to affect the shape of the excitation response spectrum in K7.

For four samples, the initial decay rate of luminescence after the excitation was switched on was found to be proportional to the initial intensity squared over the range 1.24–2.4 eV for the excitation photons.

All this information is strongly indicative that excitation occurs from only one type of trap over the range 1.24–2.4 eV; this includes the main resonance at 1.44 eV and subsidiary ones at ∼1.57 and ∼2 eV. This implies that direct excitation to the conduction band requires photons of energies greater than 2.5 eV.

Acknowledgments

The following are thanked for providing samples or help with collecting them: M Auclair, W Blake, J J Clague, S R Dallimore, R J Fulton, L Groat, S R Hicock, H Jungner, M Lamothe, O B Lian, Y A Mochanov, J Ollerhead, P A Shane, M A Short, P Soloveyeev, S van Heteren and S A Wolfe. This research was supported by the Natural Sciences and Engineering Research Council of Canada.

References

Aitken M J 1998 *An Introduction to Optical Dating* (Oxford: Oxford University Press)
Bailiff I K and Barnett S M 1994 *Radiat. Meas.* **23** 541–5
Baril M R 1997 Optical dating of tsunami deposits *MSc Thesis* Simon Fraser University, Burnaby, BC, Canada
Baril M R 2004 CCD imaging of the infrared stimulated luminescence of feldspars *Radiat. Meas.* at press
Baril M R and Huntley D J 2003 Infra-red stimulated luminescence and phosphorescence spectra of irradiated feldspars *J. Phys.: Condens. Matter* **15** 8029–48
Barnett S M and Bailiff I K 1997 *Radiat. Meas.* **27** 237–42
Bøtter-Jensen L, Duller G A T and Poolton N R J 1994 *Radiat. Meas.* **23** 613–6
Di Bartolo B 1968 *Optical Interactions in Solids* (New York: Wiley)
Di Bartolo B and Powell R C 1976 *Phonons and Resonances in Solids* (New York: Wiley)
Ditlefsen C and Huntley D J 1994 *Radiat. Meas.* **23** 675–82
Godfrey-Smith D I and Cada M 1996 *Radiat. Prot. Dosim.* **66** 379–85
Hofmeister A M and Rossmann G R 1984 *Phys. Chem. Minerals* **11** 213–24
Huntley D J, Godfrey-Smith D I and Thewalt M L W 1985 *Nature* **313** 105–7
Huntley D J, Short M A and Dunphy K 1996 *Can. J. Phys.* **74** 81–91
Hütt G, Jaek I, Brodski L and Vasilchenko V 1999 *Appl. Radiat. Isot.* **50** 969–74
Hütt G, Jaek I and Tchonka J 1988 *Quat. Sci. Rev.* **7** 381–5
Krbetschek M R, Götze J, Dietrich A and Trautmann T 1997 *Radiat. Meas.* **27** 695–748
Kurik M V 1971 *Phys. Status Solidi* **8** 9–45
McKeever S W S, Bøtter-Jensen L, Agersnap Larsen N and Duller G A T 1997 *Radiat. Meas.* **27** 161–70
Ollerhead J, Huntley D J, Nelson A R and Kelsey H M 2001 *Quat. Sci. Rev.* **20** 1915–26
Poolton N R J, Bøtter-Jensen L and Johnsen O 1995 *Radiat. Meas.* **24** 531–4
Poolton N R J, Bøtter-Jensen L, Ypma P J M and Johnsen O 1994 *Radiat. Meas.* **23** 551–4
Short M A 2003 An investigation into the physics of the infrared excited luminescence of irradiated feldspars *PhD Thesis* Simon Fraser University, Burnaby, BC, Canada
Short M A and Huntley D J 2000 *Radiat. Meas.* **32** 865–71
Trautmann T, Krbetschek M R and Stolz W 2000 *Radiat. Meas.* **32** 685–90